Histol Histopathol (2004) 19: 677-685

http://www.hh.um.es

Histology and Histopathology

Cellular and Molecular Biology

Ultrastructural changes in bones of the senescence-accelerated mouse (SAMP6): a murine model for senile osteoporosis

H. Chen[1], S. Shoumura[1] and S. Emura[2]

[1]Department of Anatomy, Gifu University School of Medicine, Gifu, Japan and

[2]Nursing Course, Gifu University School of Medicine, Gifu, Japan

Summary. SAMP6, a substrain of senescence-accelerated mice, was developed as an animal model for senile osteoporosis. In the present study, we investigated the bone morphology, together with serum calcium and bone mineral density (BMD) in SAMP6 and age-matched normal mice SAMR1. We did not find any significant differences between SAMR1 and SAMP6 at 1 month of age with regard to the serum compositions and bone morphology. As compared with SAMR1, BMD, the femoral weight, femoral calcium and phosphorus levels were significantly reduced in SAMP6 at 2 and 5 months of age. The number of osteoblasts in trabecular bones was also significantly reduced. Swollen mitochondria and myelin-like structures were found in osteoblasts and osteocytes of SAMP6 mice at 2 and 5 months of age. There was a greater proportion of resting surface and less forming surface in the femoral endosteal surfaces of SAMP6 mice. The amount of trabecular bone in the lumbar vertebra and the distal metaphysis of the femur was reduced. The number of the mast cells in bone marrow of the tibia significantly increased in SAMP6 mice. These findings indicate that the lower bone mass in SAMP6 was due to the reduction in osteoblast formation and suggested that mast cells in bone marrows play a role in the pathogenesis of senile osteoporosis.

Key words: SAMP6, Bone, Mast cell, Ultrastructure, Histomorphometry

Introduction

The human skeleton is continually renewed by osteoclasts and osteoblasts, the two specialized cell types. An orderly supply of osteoclasts and osteoblasts is essential for skeletal homeostasis, as changes in their number, morphology and function are responsible for the mismatch between bone resorption and formation that underlies most bone diseases, including osteoporosis (Jilka et al., 1996). Osteoporosis is becoming a major public health problem in all developed countries. Despite numerous investigations, the pathogenesis, treatment and prevention of osteoporosis remain unsolved problems. There are few data on age-related bone changes in experimental animals (Kiebzak et al., 1988). Takeda and his colleagues established the experimental model of senescence-accelerated mice (SAM), which consists of SAMP and SAMR series (Takeda et al., 1981). Aging is accelerated in SAMP mice as compared with normal SAMR mice. SAMP6 mice have been reported to be the first spontaneous experimental model for senile osteoporosis (Matsushita et al., 1986). These mice exhibit a decrease in bone mass and bone formation early in life when compared with their normal controls, SAMR1 (Tsuboyama et al., 1989). In experiments with SAMP6 and SAMP2, it was reported that the number of osteoclasts per unit bone surface length and the osteoclast surface in SAMP6 significantly increased. Furthermore, the ratio of osteoclast/TRAP-positive cells free in the bone marrow cavity was higher in SAMP6 than in SAMP2. Activated bone resorption may play a role in the osteoporosis seen in SAMP6 mice (Okamoto et al., 1995). Bone marrow is the principal site for osteoclastogenesis and osteoblastogenesis. It has been recently demonstrated by using light microscopy and the histomorphometric method that both osteoclastogenesis and osteoblastogenesis decreased in SAMP6 mice (Jilka et al., 1996; Kajkenova et al., 1997; Kodama et al., 1998). However, few data are available concerning the ultrastructural aspect of the bone in SAMP6 mice. The purpose of the present study was to compare the morphological, especially the ultrastructural, changes of the bone and bone marrow between SAMP6 and SAMR1 mice.

Materials and methods

SAMP6/Ta and SAMR1/Ta mice were kindly donated by the Council for SAM Research, Kyoto,

Offprint requests to: Dr. Huayue Chen, Department of Anatomy, Gifu University School of Medicine, 40 Tsukasa-machi, Gifu 500-8705, Japan. Fax: +81-58-267-2218. e-mail: huayue@cc.gifu-u.ac.jp

Japan. Animals were maintained under conventional conditions and had free access to tap water and commercial diet (CE-2, CLEA Japan). In this study, we used 1-, 2- and 5-month-old mice of both SAMP6 and SAMR1 in groups of 15 each totaling 90 animals.

The bone mineral density (BMD) of the whole body was measured by Dual Energy X-ray Absorptiometry (DXA) using a type 2000 Toyo Medic QDR. The blood was taken from the heart under ether anesthesia. The serum calcium and phosphorus levels were determined by the standard colorimetric method, as described previously (Chen et al., 2002).

The femurs, tibias, lumbar vertebrae and parietal bones were dissected and cleaned of soft tissue. Femurs were heated at 120 °C for 3 hours. The femoral length was measured from the tip of the greater trochanter to the distal surface of the condyle. The dry weight of the femur was measured on a precision balance. The dried femurs were pulverized and each aliquot of the bone powder was hydrolyzed in 6N HCl at 150 °C for 3 hours. After neutralization, the femoral calcium and phosphorus levels were determined by the colorimetric methods described above.

Some femurs and the third lumbar vertebrae from all groups were processed for scanning electron microscopy (SEM). The distal part of the femur and the vertebral body of the third lumbar vertebra were trimmed in the sagittal plane. They were treated with 5% sodium hypochlorite solution to expose the trabecular bone. The bones were then dehydrated in acetone and critical-point dried, mounted on stubs and coated with gold/palladium using an ion sputter. The bones were examined with a Hitachi S-3500 N SEM. The trabecular bone volume per tissue volume (BV/TV) was measured using an image measuring system (Finetec), according to the standard nomenclature for bone histomorphometry (Parfitt et al., 1987).

The femoral diaphyses of 5 mm-long were taken from each shaft just below the third trochanter. The endosteal surfaces were processed for SEM observation. Ten micrographs at final magnifications of 500 were taken from each animal. The percentage area of forming, resting and resorbing surfaces were estimated using an image measuring system (Finetec). Types of bone surfaces have been described extensively (Wink, 1982; Chen et al., 2002). In the present study, the following types were analyzed: (1) forming surfaces composed of mineral nodules, indicative of bone-forming surfaces in various stages of mineralization; (2) resting surfaces composed of mineralized collagen fibers, indicative of completely mineralized resting bone surfaces; and (3) resorbing surfaces showing depressions or pits with bright scalloped edges, indicative of osteoclastic resorptions.

The osteocytes of the parietal bones were investigated by the EDTA-KOH method, as previously reported (Abe et al., 1992). Animals were fixed by perfusion with 2.5 % Glutaraldehyde in 0.1M cacodylate buffer at pH 7.3. The parietal bones were dissected and fixed with the same fixative overnight, then decalcified with 5% EDTA and finally digested with 30% KOH to remove the bone matrix. The bones were postfixed with 1% OsO_4 and stained with 2% tannic acid, dehydrated, and critical-point dried. The specimens were sputter-coated with gold palladium and observed with a Hitachi S-3500 N SEM.

The tibias were cut in half sagittally with a razor blade after perfusive fixation. The proximal parts of the tibia were minced and fixed with the same fixative overnight and then decalcified with 10% EDTA. The tissues were postfixed in 1% OsO_4 in 0.1 M cacodylate buffer (pH 7.3), dehydrated through ascending concentrations of acetone, and embedded in Epon 812. Semi-thin sections were stained with Azur II and observed with a light microscope (LM). The number of the mast cells was calculated in the bone marrow of the proximal metaphysis of the tibia. Mast cells were easily differentiated with Azur II staining from the other cell types on the basis of the metachromatic staining of their cytoplasmic granules. The data are expressed as cell number per mm^2 of bone marrow. The number of osteoblasts and osteoclasts was also calculated on the trabecular bones of the proximal metaphysis of the tibia. Ultrathin sections were prepared on a Porter-Blum MT-1 ultramicrotome. After being stained with uranyl acetate and lead salts, the sections were examined with a Hitachi H-800 transmission electron microscope (TEM), as previously reported (Chen et al., 2001).

All data were presented as mean±SEM. Statistical analysis was done using StatView J-4.5 (Abacus Concepts). Significance of the results was determined by one-way analysis of variance (ANOVA) and Fisher's PLSD test. A p value <0.05 was considered statistically significant.

Results

We did not find any significant differences between SAMP6 and SAMR1 mice at 1 month of age with regard to the serum calcium and phosphorus levels, the femoral calcium level, and phosphorus levels (Table 1). As compared with SAMR1, the serum calcium and

Table 1. The serum and femoral Ca and Pi levels in SAMR1 and SAMP6 mice.

AGE		SERUM Ca (mg/100 ml)	SERUM Pi (mg/100 ml)	FEMIUR Ca (mg/g)	FEMIUR Pi (mg/g)
1 m	SAMR1	9.9±0.3	10.1±0.5	233.1±5.1	123.5±10.2
	SAMP6	9.9±0.3	10.1±0.6	233.5±3.2	123.4±9.6
2 m	SAMR1	9.5±0.3	9.2±0.6	239.3±3.6	125.5±11.3
	SAMP6	9.8±0.2*	9.6±0.8*	237.4±6.9	124.6±10.7
5 m	SAMR1	9.3±0.2	7.3±0.5	226.2±5.1	119.8±10.2
	SAMP6	9.6±0.2*	8.1±0.5*	215.1±4.8*	109.5±8.7*

Values are shown as mean±SEM. *p<0.05.

phosphorus levels increased slightly but significantly in SAMP6 at 2 and 5 months of age. A significant decrease in the femoral calcium and phosphorus levels was observed in SAMP6 at 5 months of age (Table 1). The BMD of the whole body and the femoral dry weight tended to decrease in SAMP6 at 2 months of age, and this decline was significant at 5 months of age (Table 2). The trabecular bone volume in SAMP6 significantly decreased at 2 and 5 months of age (Table 2). However, the femoral shape and the femoral length of SAMP6 resembled those of SAMR1.

The SEM images of the trabecular bone in the distal

Table 2. Body weight, BMD, femoral weight, length and trabecular bone volume in SAMR1 and SAMP6 mice.

AGE		BODY WEIGHT (g)	BMD (mg/cm^2)	FEMORAL WEIGHT (mg)	FEMORAL LENGTH (mm)	BV/TV (%)
1 m	SAMR1	21.5±2.7	53.5±3.3	17.1±0.9	12.2±0.5	26.4±4.3
	SAMP6	21.3±3.5	52.7±2.2	17.2±0.8	12.3±0.9	25.9±5.1
2 m	SAMR1	26.0±4.1	62.9±4.3	29.8±1.0	14.6±0.7	25.8±3.9
	SAMP6	29.1±3.9	59.7±5.1	27.7±0.9	14.8±1.2	22.1±3.2*
5 m	SAMR1	31.4±3.8	69.3±2.9	40.4±1.5	16.9±0.8	23.5±2.6
	SAMP6	34.1±4.5	59.8±3.4*	37.9±1.7*	16.7±1.1	18.7±2.9*

Values are shown as mean±SEM. *$p<0.05$.

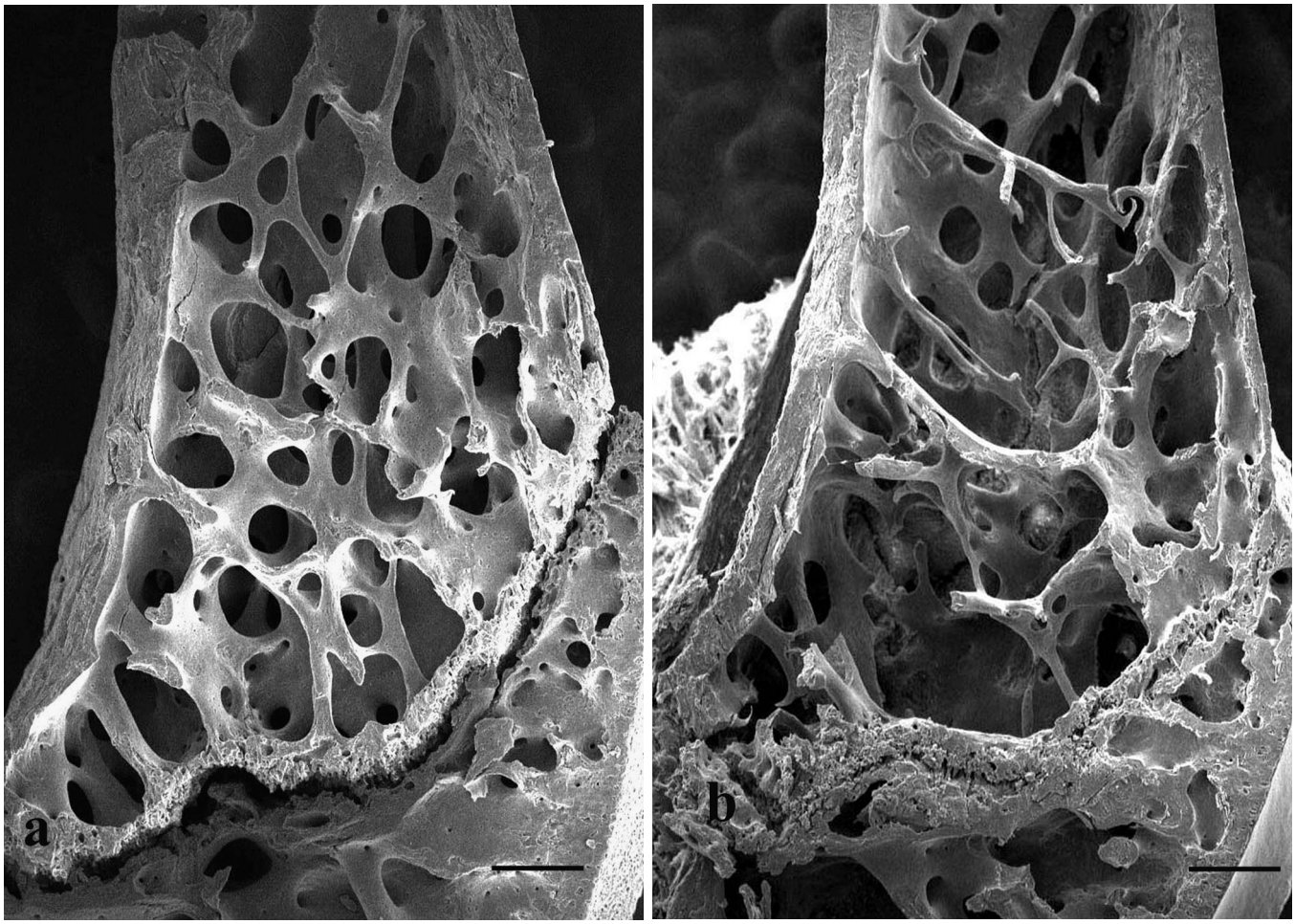

Fig. 1. Scanning electron micrographs of the distal metaphyses in mice femurs at 5 months of age. **a:** SAMR1; **b**: SAMP6. The amount of trabecular bone is reduced and the cortical bone becomes thinner in the SAMP6 mouse. Scale bar: 0.5 mm.

metaphysis of the femur and the vertebral body of the third lumbar vertebra were similar in both SAMP6 and SAMR1 at 1 month of age. The amount of trabecular bone in the metaphyseal region of the femur was clearly reduced in SAMP6 mice at 5 months of age (Fig. 1). The trabecular bone in the lumbar vertebra significantly decreased in SAMP6 mice at 5 months of age (Fig. 2). The same results were obtained with SAMP6 mice at 2 months of age. In the SEM images of the endosteal surfaces of the femoral diaphyses, we did not find any morphological changes in SAMP6 mice at 1 month of age. As compared with SAMR1, there was a lower amount of the forming surface and more resting surface and the ratio of forming/resorbing surfaces significantly decreased in SAMP6 mice at 2 and 5 months of age (Table 3, Fig. 3).

After EDTA-KOH treatment, the bone matrix was dissolved and the cellular components of the bone were observed to be almost intact in association with the undigested bone. In SAMR1 mice, most of the osteocytes were round or oval in shape. They were connected with neighboring osteocytes by numerous long and extensively branched cell processes, forming a complicated network (Fig. 4a). In SAMP6 mice at 2 and 5 months of age, many osteocytes showed a flattened appearance and some were degenerated (Fig. 4b).

The trabecular bone of the proximal tibia was observed with LM and TEM. Osteocytes, osteoblasts

Table 3. Bone surface types on endosteal surface of the femoral diaphysis.

AGE		FORMING (%)	RESTING (%)	RESORBING (%)	FORMING/ RESORBING
1 m	SAMR1	18.7±4.8	57.9±15.6	23.4±7.1	0.80±0.13
	SAMP6	18.1±5.2	59.3±22.5	22.6±6.5	0.80±0.09
2 m	SAMR1	16.1±5.7	64.1±17.4	19.8±7.4	0.81±0.10
	SAMP6	11.3±4.3*	72.2±24.4	16.5±5.9	0.68±0.08*
5 m	SAMR1	12.3±2.5	66.5±12.7	21.2±6.4	0.58±0.07
	SAMP6	5.7±3.8*	79.1±15.0	15.2±5.5	0.37±0.05*

Values are shown as mean±SEM. *p<0.05.

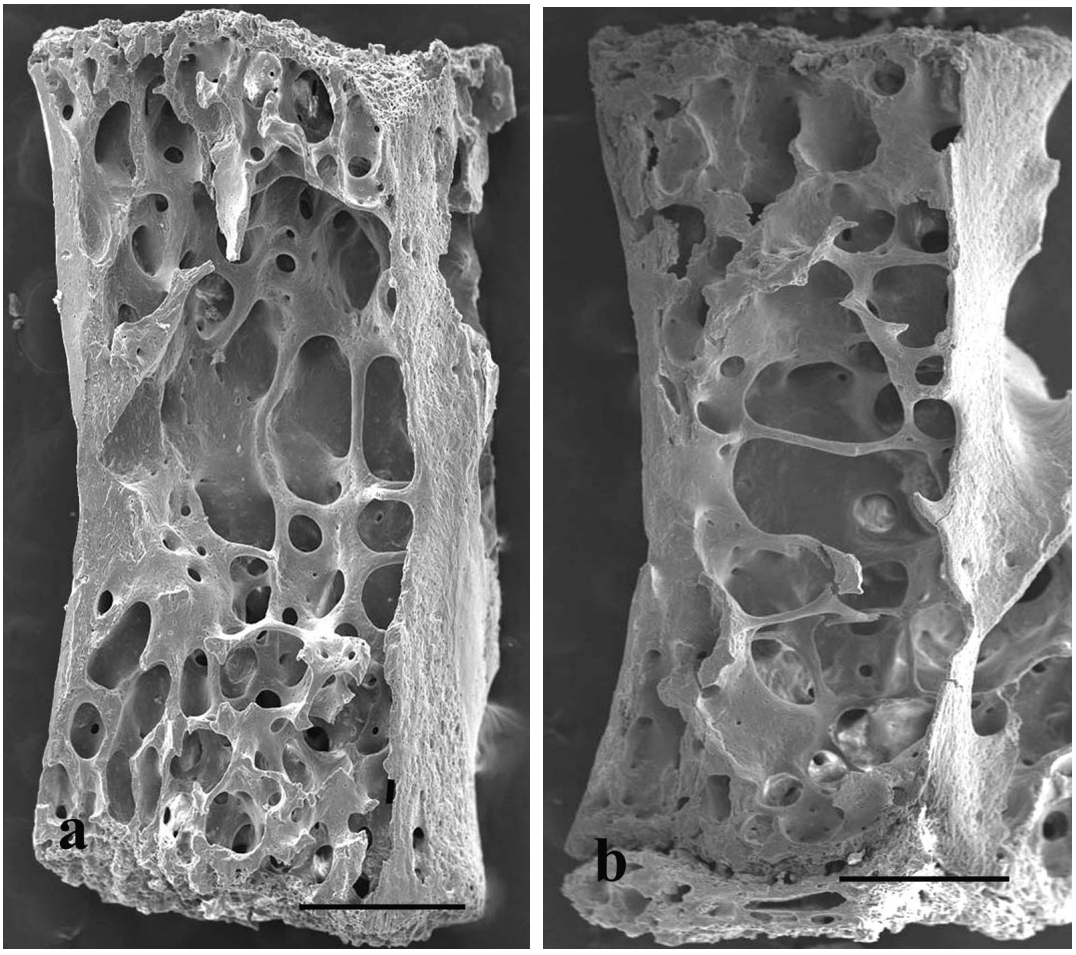

Fig. 2. Scanning electron micrographs of the vertebral body in the third lumbar vertebra of the mice at 5 months of age. **a:** SAMR1; **b:** SAMP6. The trabecular bone is decreased in the SAMP6 mice. Scale bar: 0.5 mm.

and osteoclasts of the tibia are easily identified in Azur II-stained sections. The osteoblast number of the trabecular bone in SAMP6 mice at 5 months of age significantly decreased (Table 4). There was no significant difference between SAMP6 and SAMR1 with regard to the number of osteoclasts (Table 4).

Osteocytes in SAMR1 mice were smaller and had a narrow rim of cytoplasm with only a few mitochondria and very few cisternae of granular endoplasmic reticulum. Mitochondria appeared normal, with apparent cristae (Fig. 5a). Osteocytes were situated in the lacunae within bone and were connected to adjacent cells by

Table 4. The number of trabecular osteoblasts, osteoclasts and bone marrow mast cells in femurs.

AGE		NUMBER OF OSTEOBLASTS (per mm^2)	NUMBER OF OSTEOCLASTS (per mm^2)	NUMBER OF MAST CELLS (per mm^2))
1 m	SAMR1	38.2±8.9	2.0±0.5	2.2±0.4
	SAMP6	36.7±9.6	2.3±0.7	2.3±0.5
2 m	SAMR1	44.8±10.5	1.9±0.6	2.5±0.7
	SAMP6	41.0±11.7	1.5±0.4	7.6±0.5*
5 m	SAMR1	45.1±16.3	1.6±0.6	3.7±0.6
	SAMP6	27.7±13.5*	1.2±0.5	13.1±2.8*

Values are shown as mean±SEM. *p<0.05.

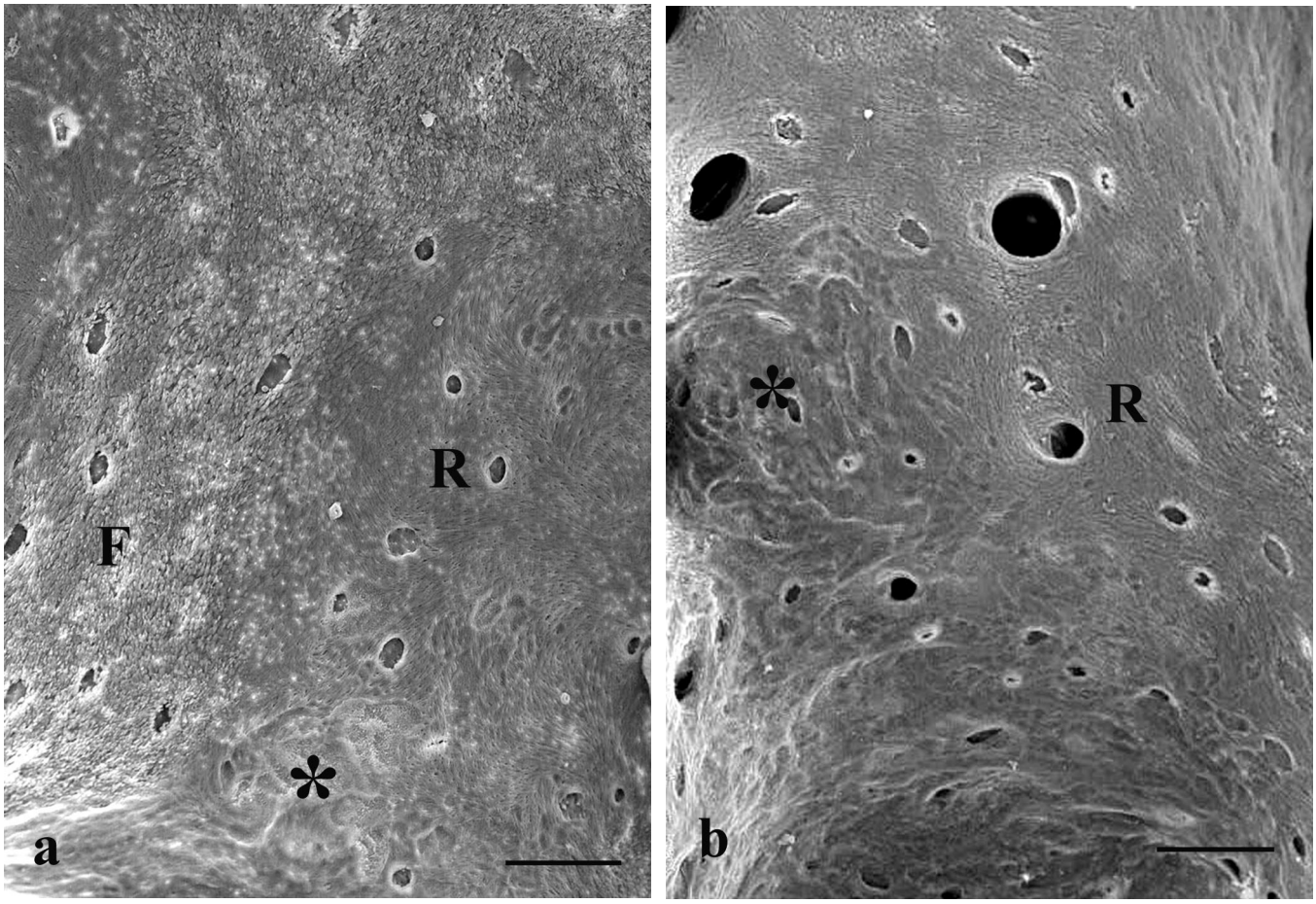

Fig. 3. Scanning electron micrographs of the endosteal surfaces in femoral diaphyses at 5 months of age. **a:** SAMR1; **b:** SAMP6. Note more resting surface (R) and less forming surface (F) in the SAMP6 mouse. Asterisk: resorbing surface. Scale bar: 50 μm.

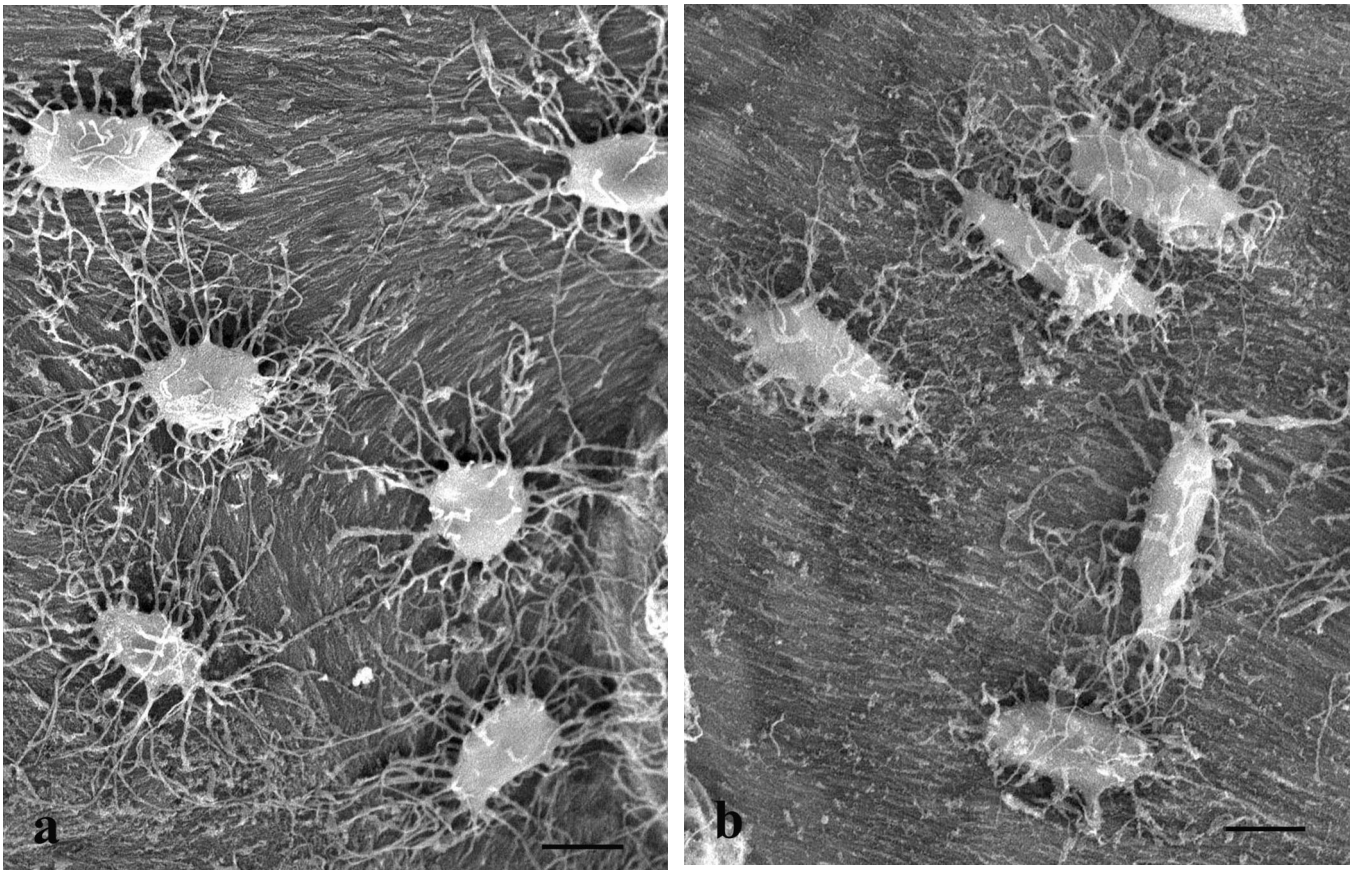

Fig. 4. Scanning electron micrographs of osteocytes from mice parietal bones at 5 months of age. **a:** SAMR1; **b:** SAMP6. Osteocytes are round or oval in shape. They are connected with neighboring osteocytes by numerous long and extensively branched cell processes in the SAMR1 mouse. Many osteocytes show a flattened appearance in the SAMP6 mouse. Scale bar: 10 μm.

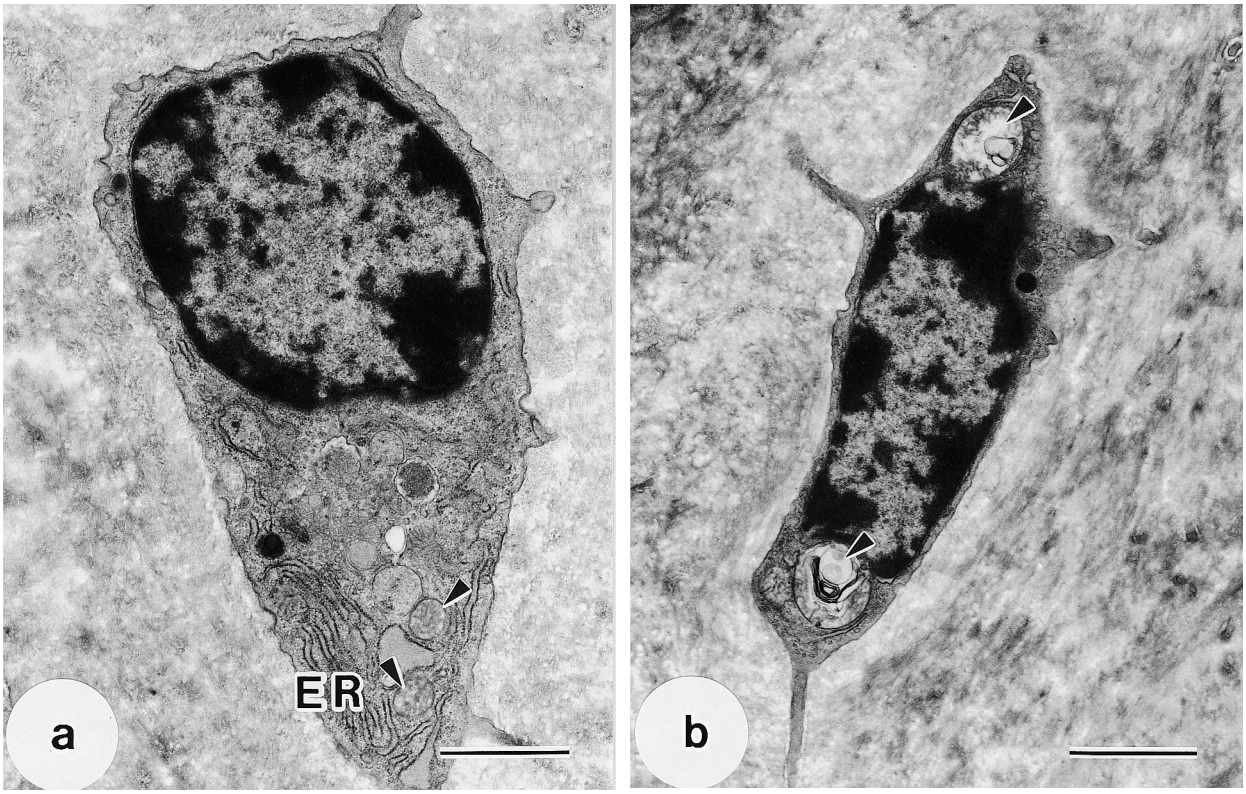

Fig. 5. Transmission electron micrographs of the tibial osteocytes in mice at 5 months of age. **a:** SAMR1; **b:** SAMP6. Abundant cisternae of the granular endoplasmic reticulum (ER) are observed in the cytoplasm. Mitochondria (arrowheads) appear normal in the SAMR1 mouse. Mitochondria (arrowheads) are swollen and disrupted in the flattened osteocyte in the SAMP6 mouse. Scale bar: 2 μm.

numerous long cytoplasmic projections, which traveled in canaliculi through a mineralized matrix (Fig. 5a). The osteocytes in SAMP6 at 2 and 5 months of age showed a slightly flattened appearance. Some mitochondria were swollen, disrupted and demonstrated vacuolization (Fig. 5b). In the SAMR1 mice, the osteoblasts had abundant cisternae of granular endoplasmic reticulum and prominent well-developed Golgi complexes. Mitochondria were large, with well-developed cristae (Fig. 6a). Most mitochondria appeared healthy and intact (Fig. 6a). The ultrastructure of the osteoblasts in SAMP6 at 1 month of age was similar to that of the SAMR1. In SAMP6 at 2 and 5 months of age, the osteoblasts contained abundant granular endoplasmic reticulum. Mitochondria demonstrated pronounced vacuolization and some were uniformly swollen and disrupted (Fig. 6b). Myelin-like structures were sometimes found in osteoblasts of SAMP6 at 2 and 5 months of age (Fig. 6c). The morphology of the osteoclasts in SAMP6 resembled that of SAMR1. There were no swollen mitochondria in osteoclasts of either SAMR1 or SAMP6 animals.

The bone marrow of the proximal tibia exhibited a striking increase in the mast cell population in SAMP6 mice at 2 and 5 months of age (Table 4, Fig. 7). Ultrastructurally, we found numerous mast cells were in close proximity to osteoblast progenitors (Fig. 7). Some of them showed degranulating.

Discussion

The structure of the bone is maintained by a delicate relationship between bone resorption and formation. In healthy adults, the amount of bone formation by osteoblast approximately balances the amount of bone resorption by osteoclasts. In aged individuals, the balance shifts to favor bone resorption, which can result in debilitating diseases such as osteoporosis. Theoretically, bone loss could arise from a reduction in

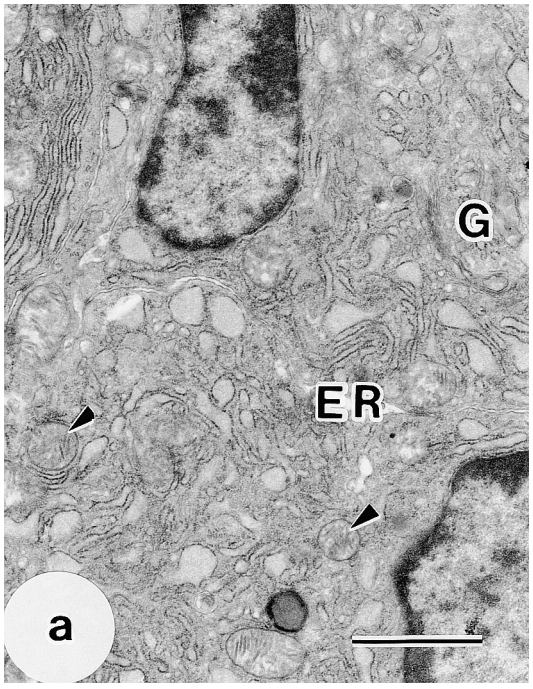

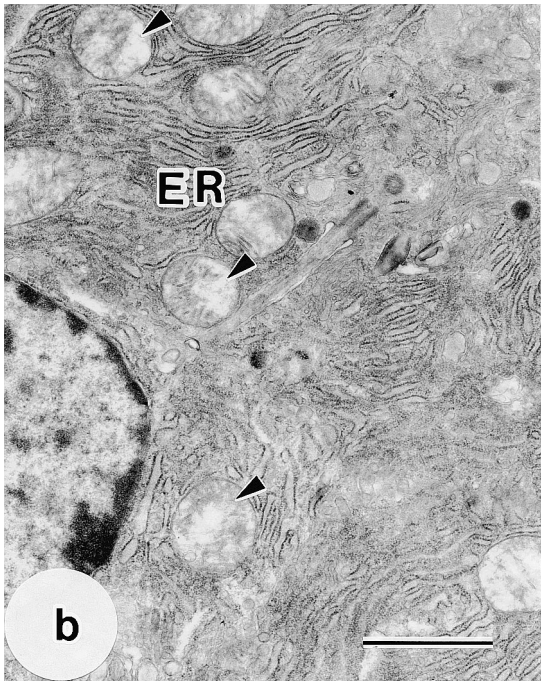

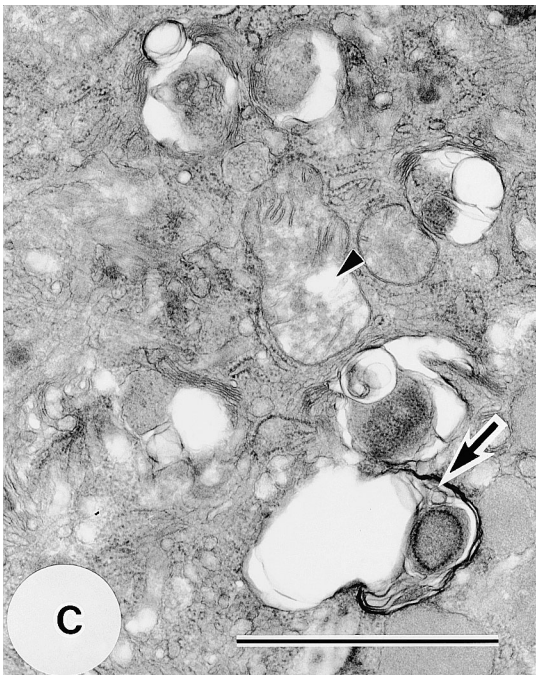

Fig. 6. Transmission electron micrographs of the tibial osteoblasts in mice at 5 months of age. **a:** SAMR1; **b, c:** SAMP6. Abundant cisternae of the granular endoplasmic reticulum (ER), well-developed Golgi complex (G) and normal mitochondria (arrowheads) are observed in the cytoplasm in the SAMR1 mouse. Swollen mitochondria (arrowhead) and a myelin-like structure (arrow) are found in the osteoblasts of the SAMP6 mouse. Scale bar: 2 μm.

the number and function of osteoblasts or an increase in bone resorption.

A tetracycline-labeled photometric assay has demonstrated that the bone formation at the femoral endosteal surface was significantly decreased in SAMP6 mice at the age of 28 days to 60 days (Tsuboyama et al., 1989). Results from chemical analysis of the bone, urine and serum showed that bone resorption were accelerated in SAMP6 mice (Kawase et al., 1989). A bone histomorphometric study indicated that the number and surface length of osteoclasts increased in SAMP6 mice, as compared with SAMP2, not SAMR1 mice (Okamoto et al., 1995). Activated bone resorption may play a role in the pathogenesis of bone loss seen in SAMP6. Evidence obtained recently has strongly suggested that the bone defect exhibited by SAMP6 mice is due to a premature decrease in the ability of mesenchymal progenitors of the bone marrow to differentiate toward the osteoblasts (Jilka et al., 1996; Kajkenova et al., 1997; Kodama et al., 1998).

The present study demonstrated that SAMP6 and SAMR1 mice at 1 month of age had identical numbers of osteoblasts, a similar area of bone forming surface and a comparable BMD. However, SAMP6 mice at 2 and 5 months of age showed a significant decrease in the number of osteoblasts, and this decline was accompanied by a reduction in the area of the bone forming surface and trabecular bone volume, diminished bone mass and ultrastructural changes of osteoblasts. The ratio of the bone forming surface to the resorbing surface decreased, though we did not find any significant changes in the number and morphology of osteoclasts in SAMP6 mice. We consider that the bone loss in SAMP6 mice mainly arises from the decreased bone formation due to the reduction in the number and function of osteoblasts.

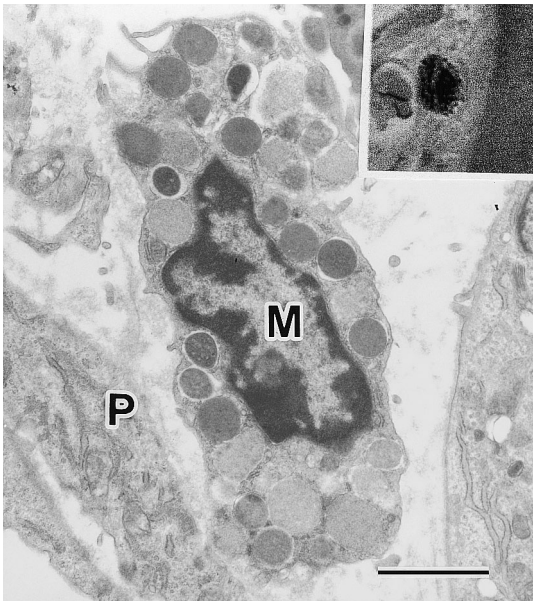

Fig. 7. Transmission electron micrograph of bone marrow mast cell in a SAMP6 mouse at 5 months of age. A mast cell (M) is in close proximity to an osteoblast progenitor (P). Scale bar: 2 μm. Insert: Light micrograph of a bone marrow mast cell adjacent to the bone surface.

Histomorphometric analyses revealed a decline in trabecular bone with a reduction in the number and function of osteoblasts in age-related bone loss (Parfitt et al., 1995). Thus, a reduction in bone formation due to a decrease in the recruitment of osteoblasts is the principal feature of senile osteoporosis, although an age-related decrease in the activation of vitamin D and an increase in parathyroid hormone (PTH) may cause a rise in bone resorption (Eastell et al., 1991). Roholl et al. (1994) suggested that age-related bone loss in rats resulted from an imbalance between bone resorption and formation. Of these two processes, the decreased bone formation due to a diminished number and ultrastructural changes of osteoblasts appeared to be the major factor.

A number of factors produced in the bone marrow microenvironment are capable of influencing the development, differentiation and function of osteoblasts and osteoclasts (Mundy et al., 1995). Previous in vitro studies showed that the production and the action of IL-11 were deficient, and those of IL-6 increased in bone marrow cells of SAMP6 mice (Kajkenova et al., 1997; Kodama et al., 1998). Alternations of cytokines in bone marrow might cause the disturbances in the differentiation of bone marrow stromal cells to osteoblasts, resulting in bone loss. There is evidence that mast cells of the bone marrow release biological mediators potentially involved in bone metabolism, such as heparin, histamine, IL-1, IL-3, IL-6 and TNF (Alsina et al., 1996). An increase in the number of mast cells has been described in the bone marrow of elderly women with osteoporosis (Frame and Nixon, 1968). It has recently been suggested that mast cells in the bone marrow may be involved in the events leading to bone loss by changing bone remodeling activity (Brumsen et al., 2002). In the present study, we found that the number of mast cells in the bone marrow of SAMP6 mice at 2 and 5 months of age dramatically increased and that some of them were degranulating, i.e., they were in a state of activation. Moreover, some mast cells were in close proximity to bone surface. Because of their close spatial association with the bone cells, we consider that mast cells of the bone marrow may provide a paracrine mechanism which regulates the recruitment and function of osteoblast progenitors.

In conclusion, the present study provides evidence that the low bone mass in SAMP6 mice is mainly produced by the reduction in osteoblast function. That mast cells in the bone marrow play a role in the pathogenesis of bone loss in SAMP6 mice is at least theoretically possible.

References

Abe K., Hashizume H. and Ushiki T. (1992). An EDTA-KOH method to expose bone cells for scanning electron microscopy. J. Elect.

Microsc. 41, 113-115.

Alsina M., Guise T.A. and Roodman G.D. (1996). Cytokine regulation of bone cell differentiation. Vitam. Horm. 52, 63-98.

Brumsen C., Papapoulos S.E., Lentjes E.G., Kluin P.M. and Hamdy N.A. (2002). A potential role for the mast cell in the pathogenesis of idiopathic osteoporosis in men. Bone 31, 556-561.

Chen H., Hayakawa D., Emura S., Ozawa Y., Taguchi H., Yano R. and Shoumura S. (2001). Effects of ethanol on the ultrastructure of the hamster femur. Histol. Histopathol. 16, 763-770.

Chen H., Hayakawa D., Emura S., Ozawa Y., Okumura T. and Shoumura S. (2002). Effect of low or high dietary calcium on the morphology of the rat femur. Histol. Histopathol. 17, 1129-1135.

Eastell R., Yergey A.L., Vieira N.E., Cedel S.L., Kumar R. and Riggs B.L. (1991). Interrelationship among vitamin D metabolism, true calcium absorption, parathyroid function, and age in women: evidence of an age-related intestinal resistance to 1,25-dihydroxyvitamin D action. J. Bone Miner. Res. 6, 125-132.

Frame B. and Nixon R.K. (1968). Bone-marrow mast cells in osteoporosis of aging. N. Engl. J. Med. 279, 626-630.

Jilka R.L., Weinstein R.S., Takahashi K., Parfitt A.M. and Manolagas S.C. (1996). Linkage of decreased bone mass with impaired osteoblastogenesis in a murine model of accelerated senescence. J. Clin. Invest. 97, 1732-1740.

Kajkenova O., Lecka-Czernik B., Gubrij I., Hauser S..P, Takahashi K., Parfitt A.M., Jilka R.L., Manolagas S.C. and Lipschitz D.A. (1997). Increased adipogenesis and myelopoiesis in the bone marrow of SAMP6, a murine model of defective osteoblastogenesis and low turnover osteopenia. J. Bone Miner. Res. 12, 1772-1779.

Kawase M., Tsuda M. and Matsuo T. (1989). Accelerated bone resorption in senescence-accelerated mouse (SAM-P/6). J. Bone Miner. Res. 4, 359-364.

Kiebzak G.M., Smith R., Gundberg C.C., Howe J.C. and Sacktor B. (1988). Bone status of senescent male rats: chemical, morphometric, and mechanical analysis. J. Bone Miner. Res. 3, 37-45.

Kodama Y., Takeuchi Y., Suzawa M., Fukumoto .S, Murayama H., Yamato H., Fujita T., Kurokawa T. and Matsumoto T. (1998). Reduced expression of interleukin-11 in bone marrow stromal cells of senescence-accelerated mice (SAMP6): relationship to osteopenia with enhanced adipogenesis. J. Bone Miner. Res. 13, 1370-1377.

Matsushita M., Tsuboyama T., Kasai R., Okumura H., Yamamuro T., Higuchi K., Higuchi K., Kohno A., Yonezu T., Utani A., Umezawa M. and Takeda T. (1986). Age-related changes in bone mass in the senescence-accelerated mouse (SAM): SAM-R/3 and SAM-P/6 as new murine models for senile osteoporosis. Am. J. Pathol. 125, 276-283.

Mundy G.R., Boyce B., Hughes D., Wright K., Bonewald L., Dallas S., Harris S., Ghosh-Choudhury N., Chen D. and Dunstan C. (1995). The effects of cytokines and growth factors on osteoblastic cells. Bone 17, 71S-75S.

Okamoto Y., Takahashi K., Toriyama K., Takeda N., Kitagawa K., Hosokawa M. and Takeda T. (1995). Femoral peak bone mass and osteoclast number in an animal model of age-related spontaneous osteopenia. Anat. Rec. 242, 21-28.

Parfitt A.M., Drezner M.K., Glorieux F.H., Kanis J.A., Malluche H., Meunier P.J., Ott S.M. and Recker R.R. (1987). Bone histomorphometry: standardization of nomenclature, symbols, and units. Report of the ASBMR Histomorphometry Nomenclature Committee. J. Bone Miner. Res. 2, 595-610.

Parfitt A.M., Villanueva A.R., Foldes J. and Rao DS. (1995). Relations between histologic indeces of bone formation: implications for the pathogenesis of spinal osteoporosis. J. Bone Miner. Res. 10, 466-473.

Roholl P.J.M., Blauw E., Zurcher C., Dormans J.A.M.A. and Theuns H.M. (1994). Evidence for a diminished maturation of preosteoblasts into osteoblasts during aging in rats: an ultrastructural analysis. J. Bone Miner. Res. 9, 355-366.

Takeda T., Hosokawa M., Takeshita S., Irino M., Higuchi K., Matsushita T., Tomita Y., Yasuhira K., Hamamoto H., Shimizu K., Ishii M. and Yamamuro T. (1981). A new murine model of accelerated senescence. Mech. Ageing Dev. 17, 183-194.

Tsuboyama T., Takahashi K., Matsushita M., Okumura H., Yamamuro T., Umezawa M. and Takeda T. (1989). Decreased endosteal formation during cortical bone modelling in SAM-P/6 mice with a low peak bone mass. Bone Miner. 7, 1-12.

Wink C.S. (1982). Scanning electron microscopy of castrate rat bone. Calcif. Tissue Int. 34, 547-552.

Accepted December 29, 2003